

SDSS J123813.73-033933.0, a cataclysmic variable evolved beyond the period minimum.

A. Aviles¹, S. Zharikov¹, G. Tovmassian¹, R. Michel¹, M. Tapia¹,

*Instituto de Aatronomía, Universidad Nacional Autónoma de México, Apartado Postal 877,
22800, Ensenada, BC, México*

M. Roth²,

Las Campanas Observatory, Carnegie Institutio of Washington, Casilla 601, La Serena, Chile

V. Neustroev³,

Centre for Astronomy, National University of Ireland, Galway, Newcastle Rd., Galway, Ireland

C. Zurita⁴,

Instituto de Astrofisica de Canarias, c/ via Lactea s/n, La Laguna, E38200, Tenerife, Spain

M. Andreev⁵, A. Sergeev⁵,

Institute of Astronomy, Russian Academy of Sciences, Terskol, Russia

E. Pavlenko⁶,

Crimean Astrophysical Observatory, Nauchny, Ukraine

V. Tsymbal⁷,

Tavrian National University, Dep. Astronomy, Simferopol, Ukraine

G.C. Anupama⁸, U.S. Kamath⁸, D.K. Sahu⁸

Indian Institute of Astrophysics – CREST, Bangalore 560 034, India

¹Instituto de Aatronomía, Universidad Nacional Autónoma de México, Apartado Postal 877, 22800, Ensenada, BC, México

²Las Campanas Observatory, Carnegie Institutio of Washington, Casilla 601, La Serena, Chile

³Centre for Astronomy, National University of Ireland, Galway, Newcastle Rd., Galway, Ireland

⁴Instituto de Astrofisica de Canarias, c/ via Lactea s/n, La Laguna, E38200, Tenerife, Spain

⁵Institute of Astronomy, Russian Academy of Sciences, Terskol, Russia

⁶Crimean Astrophysical Observatory, Nauchny, Ukraine

⁷Tavrian National University, Dep. Astronomy, Simferopol, Ukraine

⁸Indian Institute of Astrophysics, II Block Koramangala, Bangalore 560034, India

ABSTRACT

We present infrared JHK photometry of the cataclysmic variable SDSS J123813.73-033933.0 and analyze it along with optical spectroscopy, demonstrating that the binary system is most probably comprised of a massive white dwarf with $T_{\text{eff}} = 12000 \pm 1000$ K and a brown dwarf of spectral type L4. The inferred system parameters suggest that this system may have evolved beyond the orbital period minimum and is a bounce-back system.

SDSS J123813.73-033933.0 stands out among CVs by exhibiting the cyclical variability that Zharikov et al. (2006) called *brightenings*. These are not related to specific orbital phases of the binary system and are fainter than dwarf novae outbursts, that usually occur on longer timescales. This phenomenon has not been observed extensively and, thus, is poorly understood. The new time-resolved, multi-longitude photometric observations of SDSS J123813.73-033933.0 allowed us to observe two consecutive *brightenings* and to determine their recurrence time. The period analysis of all observed *brightenings* during 2007 suggests a typical timescale that is close to a period of ~ 9.3 hours. However, the *brightenings* modulation is not strictly periodic, possibly maintaining coherence only on timescales of several weeks. The characteristic variability with double orbital frequency that clearly shows up during *brightenings* is also analyzed.

The Doppler mapping of the system shows the permanent presence of a spiral arm pattern in the accretion disk. A simple model is presented to demonstrate that spiral arms in the velocity map appear at the location and phase corresponding to the 2:1 resonance radius and constitute themselves as a double-humped light curves. The long-term and short-term variability of this CV is discussed together with the spiral arm structure of an accretion disk in the context of observational effects taking place in bounce-back systems.

Subject headings: stars: novae, cataclysmic variables — stars: dwarf novae — stars: brown dwarfs — stars: individual: SDSS J123813.73-033933.0

1. Introduction

The object catalogued as SDSS J123813.73-033933.0 (hereafter SDSS 1238) was identified with a faint ($r = 17.82$ mag) short-period cataclysmic variable (CV) by Szkody et al. (2003). The optical spectrum of SDSS 1238 shows a blue continuum with broad absorption features originating in the photosphere of a white dwarf surrounding double-peaked Balmer emission lines, formed in a high inclination accretion disk. The orbital period of the system is $P_{\text{orb}} = 0.05592(35)d = 1.34(1)h$, based on spectroscopic data (Zharikov et al. 2006). The orbital period and the spectral features match those of WZ-Sge-type systems, but with this, similarities practically end. A number of observed aspects of the system differ from the majority of short period CVs. The most intriguing

characteristic, which we found in this system, is a sudden and fast rise in brightness up to ~ 0.45 mag during a short time, of about half of the orbital period. After reaching its peak, the brightness slowly decreases, lasting $\sim 3 - 4$ hours, down to the quiescence level. We call these events *brightenings* in order to distinguish them from the more common outbursts, humps, flickering and other types of variability documented in short period CVs. These *brightenings* seemed to happen cyclically about every 8-12 hours. In addition to *brightenings*, a nearly permanent sinusoidal variability was detected in the light curve of SDSS 1238 with a period half that of the spectroscopic orbital period $P = P_{orb}/2 = 40.25min$ (hereafter, the double-humped light curve). The amplitude of the double-hump variability depends on the phase of the *brightenings*. It increases with a total rise in brightness of up to ~ 0.2 mag and decreases until almost disappears during the quiescence (Zharikov et al. 2006). A similar behavior was found later by Szkody et al. (2006) in another short period CV, SDSS J080434.20+510349.2 (hereafter SDSS 0804) which has an identical spectral appearance to SDSS 1238 in quiescence. Zharikov et al. (2006, 2008) advanced the hypothesis that the double-humped light curve is a signature of 2:1 resonance in the accretion disks of these systems. In order for the accretion disk to reach permanently the 2:1 resonance radius, the mass ratio of the binary component must be extreme ($q \leq 0.1$), and as such these objects could qualify as bounce-back systems, e.g. CVs, which are old enough to reach the period minimum and leap toward slightly longer orbital periods, as predicted by Paczynski (1981). It is supposed that accretion disks of WZ Sge systems reach 2:1 resonance radius during super-outburst, when some of them have been noted to show double-humped light curves (Patterson et al. 2002). The super-outbursts of WZ Sge type systems are infrequent and happen every two dozen or more years. Oddly enough, SDSS 0804 went into the super-outburst in 2006 (Pavlenko et al. 2007) and exhibited all necessary attributes of a classical WZ Sge-type object. Regrettably, the *brightenings* disappeared from the light curves of SDSS 0804 after the super-outburst, although the double-hump light curve persists (Zharikov et al. 2008). Thus, the SDSS 1238 remains the only object that still shows *brightenings*. Intrigued by the new photometric phenomenon observed in these two systems, we conducted a new time-resolved photometric study of SDSS 1238 to establish the reasons behind their common nature, understand the origin of the cyclic *brightenings* and its relation to the amplitude of the double-humped light curve. Meanwhile, we discovered that SDSS 1238 was marginally detected as an infrared source by 2MASS survey, and secured accurate near-IR photometry of the object. In Sect.2 we describe our observations and data reductions. The data analyses and the results are presented in Sects.3,4,5, while a general discussion and conclusions are given in Sect.6.

2. Observations and data reduction

The object is listed in the 2MASS¹ Point Source Catalogue with $J = 16.65(13)$, $H = 16.49(23)$, $K \sim 16.42$ magnitudes. These magnitudes are close to the detection limits of 2MASS, particu-

¹<http://www.ipac.caltech.edu/2mass/>

larly in the K -band. In order to have more accurate photometry, we obtained new observations of SDSS J123813.73-033933.0 in $J H K_s$ on 17 June 2009 with the near-infrared camera PANIC (Martini et al. 2004) attached to the 6.5 m Baade/Magellan Telescope at Las Campanas Observatory (LCO). PANIC provides an image scale of $0.125'' \text{ pixel}^{-1}$ on a Hawaii HgCdTe 1024×1024 array detector. The FWHM of the point-spread function was between $0.55''$ and $0.60''$ during our observations. For each filter, 9 dithered frames spaced by $10''$ were taken, with total on-source integration times of 540 s in each of the three filters. The nine frames were shifted and averaged to produce the final images. Standard sky-subtraction and flat-field correction procedures were applied. Aperture ($1.2''$) photometry was performed with DAOPHOT within IRAF in the standard way. Flux calibration was performed using standard stars SJ 9146 and SJ 9157 from the list of Persson et al. (1998) and the total errors are estimated to be less than 0.05 magnitudes. The resulting magnitudes of SDSS 1238 are $J = 17.07(5)$, $H = 16.65(5)$, $K = 16.42(5)$ and corresponding colors $J - H = 0.42$, $H - K_s = 0.23$ and $J - K_s = 0.65$.

In order to investigate whether flux variations in the near-IR occur in this system in timescales of a few minutes, we measured the J , H and K_s fluxes from each of the nine short-exposure (60 s) frames in each filter. In the ~ 15 min that lasted each series, we did not detect any variability within the ~ 0.15 mag photometric uncertainty associated with each single frame. Note, that in longer timescales (comparable to the orbital period), the system is expected to show some variability in the near-IR, mostly due to the elliptical shape of Roche-lobe filling secondary, but these could be missed in a 15 min time series. The ellipsoidal variability of the secondary can be calculated and it has been taken into account in further considerations of IR magnitudes.

The objective of our optical photometry of SDSS 1238 was to study of phenomenon of *brightenings*. Taking into account the long duration of the *brightenings* and the uncertainty of the cycle period (Zharikov et al. 2006), we planned and executed a multi-longitude observational campaign of this object. Time-resolved CCD photometry was obtained at several facilities: the 1.5 m telescope at the Observatorio Astronómico Nacional at San Pedro Mártir in Mexico; the 0.8 m IAC80 telescope at the Observatorio del Teide in the Canary Islands, Spain; the 2.1 m telescope at the Bohyunsan Optical Astronomy Observatory (BOAO) in South Korea; the 2m telescope at the Terskol Astrophysical Observatory in the Northern Caucasus, Russia, the 2m Himalayan Chandra Telescope of the Indian Astronomical Observatory (IAO), Hanle, India. The data reduction was performed using both ESO-MIDAS and IRAF software. The images were bias-corrected and flat-fielded before aperture photometry was carried out. The log of photometric observations is presented in Table.1.

The long-slit observations have been obtained with the Boller & Chivens spectrograph² on the 2.1-m telescope at the SPM site with a resolution of $3.03 \text{ \AA pixel}^{-1}$. The spectra span the wavelength range 4000-7100 \AA . In order to improve the signal-to-noise ratio, we obtained a series of phase-locked spectra: 10 spectra were taken at equal phase intervals over a single orbital period

²www.astrossp.unam.mx

$P_{orb} = 80.5$ min with an exposure time of 486 sec per spectrum. This sequence of spectra was repeated at exactly the same phase intervals for subsequent periods and subsequent nights. This allows us to calculate the phase-averaged spectra, summarizing the spectra of the same orbital phase obtained during one night and the whole set of observations without further decreasing the time resolution. The log of spectroscopic observations is presented in Table.2.

3. Spectral energy distribution: system parameters and distance to the object

The spectral energy distribution (SED) of the object in the range of 4000-25000Å is shown in Fig.1. The detailed description of the SDSS 1238 optical spectrum was given in our previous paper (Zharikov et al. 2006). The overall appearance of the spectrum has not changed, but we detect a significant variability of the equivalent widths of Balmer emission lines from epoch to epoch. The Balmer lines are about two times weaker in the 2009 observations compared to the 2004 spectra (Fig.2). The continuum, however, has not changed during the last five years, as we compare V-band magnitudes in quiescence between *brightenings*. The average quiescence magnitude³ between *brightenings* remains constant at around $V \cong 17.8 \pm 0.1$.

The present near-IR measurements demonstrated that there is significant IR excess emission to that expected from the Rayleigh–Jeans tail of the optical spectrum for a white dwarf (WD). In fact, neither a WD nor a power-law flux from the accretion disk, nor their combination, can explain the observed IR excess. The most probable source of IR excess is the radiation from the secondary star. To determine the spectral type of the secondary and the distance to the system we fitted the observed optical-infrared spectral energy distribution of the object with a simple model: the total flux $F^*(\lambda)$ is the sum of contributions from a WD with a hydrogen atmosphere, $F_{WD}(T_{eff}, \lambda)$ (DA type WDs), an accretion disk with $F_{AD} \sim \lambda^{-\frac{7}{3}}$ (Lynden-Bell 1969), and a red/brown dwarf with $F_{BD}(\lambda)$:

$$F^*(\lambda) = F_{WD}(T_{eff}, \lambda) + F_{AD}(\lambda) + F_{BD}^{SpT}(\lambda) \quad (1)$$

Brown dwarf fluxes were taken from the literature (McLean et al. 2003, 2007) and on-line sources⁴. The white dwarf spectra with a mass range of $M_{WD} = 0.6 - 1.1 M_{\odot}$ were used with a $0.1 M_{\odot}$ step and the radii were calculated using the white dwarf radius-mass relation of

$$R_{WD} = 1.12 \times 10^9 \left(1 - \frac{M_{WD}}{1.44 M_{\odot}} \right)^{\frac{3}{5}}$$

from Nauenberg (1972) and Warner (1995). Spectra of WDs in the 4000-25000Å range with pure hydrogen atmosphere were obtained using ATLAS9 (Kurucz 1993) and SYNTH (Piskunov 1992)

³ Secondary photometric standards were established in the field of SDSS 1238, by calibrating them using reference star S2003313360 from GSC-II www.gsss.stsci.edu/Catalogs/GCS/GSC2/GSC2.html

⁴see <http://web.mit.edu/ajb/www/browndwarfs/>

codes for an appropriate range of temperatures. Although our previous temperature estimate was $T_{\text{WD}} = 15\,600 \pm 1\,000\text{K}$ based on fits to the absorption portion of Balmer lines (Zharikov et al. 2006), in the present fitting procedure we allowed a wider temperature range from $T_{\text{eff}} = 11\,000$ to $18\,000\text{K}$, because of the larger number of free parameters. The calculations were performed with a $1\,000\text{K}$ step and with the surface gravity $g = \gamma \frac{M_{\text{WD}}}{R_{\text{WD}}^2}$. The spectra are normalized to $\lambda_0 = 5500\text{\AA}$ and the contribution of the WD is

$$F_{\text{WD}}(T_{\text{eff}}, \lambda) = C_1(\delta) * F_{\text{WD}}^{\text{norm}}(T_{\text{eff}}, \lambda),$$

where $C_1(\delta) = 10^{-0.4*(V+\delta+M_V^0)}$, $V = 17.8$ is the object's magnitude in quiescence, and δ is a parameter, determining the contribution of the flux from the WD in the V band. Finally, the $M_V^0 = 21.109$ - is the constant to convert magnitudes into flux (in $\text{ergs/cm}^2/\text{s}/\text{\AA}$) in the V band. The spectra of the accretion disk was assumed to be a simple power law

$$F_{\text{AD}}(\lambda) = (C_1(0) - C_1(\delta)) \times \left(\frac{\lambda}{\lambda_0} \right)^{-\frac{7}{3}},$$

where $(C_1(0) - C_1(\delta))$ determines the contribution from the accretion disk in the V band, assuming that the WD and the accretion disk are the only contributors in that wavelength as the only other contributor is the brown dwarf, which has a negligible flux in V.

The distance to the object is estimated to be

$$d = R_{\text{WD}} \sqrt{\frac{F^{\text{bb}}(T_{\text{eff}}, 5500\text{\AA})}{F_{\text{WD}}(5500\text{\AA})}},$$

where $F^{\text{bb}}(T_{\text{eff}}; 5500\text{\AA})$ is the black body flux at $\lambda = 5500\text{\AA}$ with effective temperature T_{eff} .

Observed SEDs of red/brown dwarfs of spectral types between M6 to L5 normalized to fit the observed flux in J were used. The bolometric correction to the J magnitude for each spectral type was taken from Tinney et al. (2003).

The free parameters of the three-component model are: the white dwarf effective temperature, T_{eff} , the mass of the white dwarf, M_{WD} , the spectral type of the secondary star, SpT, and the parameter δ (in magnitudes). The best fit model to the observed SDSS1238 spectrum in the $0.4\text{--}2.5\mu\text{m}$ range achieved for the following set of parameters (Fig.1) is: $T_{\text{WD}} = 12\,000\text{K}$, SpT = L4, $M_{\text{WD}} = 1.0M_{\odot}$ and $\delta = 0.1$. The deduced distance to the object is 110pc . We studied the behavior of χ^2 vs a single fit parameter, when the other three are fixed to their corresponding best values. Fig.3 presents χ^2 plots for various parameters with marked confidence levels corresponding to 95, 80 and 60%. We can state that χ^2 tends to the minimum value always, when $T_{\text{WD}} = 12\,000\text{K}$ and $\delta = 0.05 - 0.15$ regardless of the value of the other parameters. At the same time, there is a dependence between the mass of the WD and the spectral type of the secondary: the lower the mass, the larger the radius of WD, and thus, the larger the distance to the system, resulting in an earlier spectral type of the secondary. The best fit to the optical part of the spectrum is reached

with the mass of the WD of $M_{\text{WD}} = 1.0 M_{\odot}$, leading to the cited distance of, 110 pc, and spectral type of the secondary, L4. The entire range of secondary from $SpT = M9$ at $M_{\text{WD}} = 0.6 M_{\odot}$ and $d = 160 \text{ pc}$ to $SpT = L4$ at $M_{\text{WD}} = 1.0 M_{\odot}$, $d = 110 \text{ pc}$ was considered. However, a pronounced minimum in χ^2 for rather massive WD strongly suggests the presence of brown dwarf in this system. The indication of a massive WD is not accidental, a CV with a brown dwarf secondary, supposed to have evolved beyond minimum orbital period limit, has an age $\sim 3 - 5 \times 10^9$ years and a long history of accretion. A priori, the bounce-back CVs are assumed to harbor a massive WD, although the distribution of known masses of all WDs in eclipsing systems does not show any trend (Knigge 2006). But when considering only the short-period end of that distribution as Littlefair et al. (2008) did, then it becomes apparent that evolved systems systematically have more massive WDs. The upper limit for the mass of the secondary is $M_{\text{BD}} \leq 0.09 M_{\odot}$ for $SpT = M9$ or $M_{\text{BD}} \leq 0.07 M_{\odot}$ for $SpT = L4$ (Close et al. 2003). But it is also a well known fact that the secondaries of CVs tend to show systematically an earlier spectral class and a larger radius with secondaries of lower mass than the corresponding single stars on the main sequence (Littlefair et al. 2008). So we expect that the mass of the secondary in SDSS 1238 hovers around the lower edge of the above mentioned range of masses.

Note, that due the high galactic latitude of this object ($b = 59.5$) and the inferred small distance, the interstellar extinction is negligible. We also would like to emphasize that in the above calculations we took into account the fact that the state of the system was unknown at the moment of acquiring the IR data. Therefore, we conducted the fitting for both cases, considering that the system might have been at the maximum of the *brightenings* during the IR observations or at the bottom. That introduced only a minor change, basically decreasing the distance to the system by $\sim 15 \text{ pc}$ and not affecting our conclusions regarding the spectral type of the secondary. Finally, we would like to comment on the discrepancy in the temperature determination of the WD, which is larger than we would like as compared to that of Zharikov et al. (2006). In the latter the temperature and gravity could not be determined simultaneously, and one parameter had to be fixed in order to calculate the other, which always introduces ambiguity, as none of these two parameters could be estimated independently. In this paper we take a more complex approach: not only profiles of the lines are being fitted, but the continuum is taken into consideration as well. Also, the presence of the secondary, adding additional restraints on the distance and thus, on the size of the WD. The SED of the accretion disk, which may not necessarily obey the canonical power law index is the source of the largest uncertainty in our analysis. Since the contribution of the disk is limited to only $\leq 20 \%$, so is the accuracy of our estimates. With all that in mind, we still end up with a range of spectral classes for the secondary that implies that SDSS 1238 is a bounce-back system.

4. Doppler tomography of SDSS1238

The H_α emission line originating in the accretion disk is the least affected by the absorption from the underlying white dwarf. Therefore, we constructed Doppler maps (Marsh & Horne 1988) of H_α using all our data obtained in 2004 and 2009 (Fig.4, top). The individual maps of separate nights resemble each other so much, that combining all available data did not smooth out details, but made them much more convincing. In order to over-plot contours of the secondary star, the location of the WD, the trajectory of the stream and resonance radius of the disk, we used the best fit parameters to the SED (see previous section). Thus, the white dwarf mass of $M_{WD} = 1.0 M_\odot$ was adopted. Due to the ambiguity in determining precise masses of brown dwarfs, we adopted a mass ratio of $q = 0.05$. This value is typical for systems considered as bounce-back (Knigge 2006) and it is the same mass ratio which was obtained for SDSS0804, a twin of SDSS 1238, from the super-hump period observed during the super-outburst in 2006 (Pavlenko et al. 2007; Zharikov et al. 2008). Before SDSS 0804 underwent a WZ-Sge type super-outburst, it showed similar peculiar photometric variability to SDSS 1238. In addition, it shares every other characteristic of a WZ Sge-type object, and was also proposed as a candidate to the bounce back system (Zharikov et al. 2008).

As already noted, the structure of the accretion disk did not change between the two epochs of our observations. There is a bright spot at the expected place where the stream of matter from the secondary collides with the accretion disk, but it overlaps with a much larger and prolonged structure, too extended to be a part of the spot. Another extended bright region of similar size can be seen at velocity coordinates ($\approx 700 \text{ km s}^{-1}$, $\approx 0 \text{ km s}^{-1}$) as well as a less bright structure at ($\approx -200 \text{ km s}^{-1}$, $\approx -800 \text{ km s}^{-1}$). Similar Doppler maps were obtained for WZ Sge during super-outburst in 2001 (Baba et al. 2002; Howell et al. 2003; Steeghs 2004) and in quiescence for bounce back candidates SDSS 1035 (Southworth et al. 2006) and SDSS 0804 (Aviles et al. in preparation).

Such brightness distribution in the Doppler map can be interpreted as evidence of spiral waves in the disk (see for example, Steeghs & Stehle (1999) and Steeghs (2001) and reference therein). The formation of a spiral structure in an accretion disk of a close binary system was predicted by Lin & Papaloizou (1979) and explored by various authors (Matsuda et al. (1990); Heemskerk (1994); Stehle (1999); Kunze & Speith (2005); Truss (2007) and reference therein). Sawada et al. (1986a,b) demonstrated from high resolution numerical calculations that spirals will always formed in accretion disks under tidal forces from the secondary. They actually used $q = 1$ in their models, but observationally, such spirals were detected in a number of systems only during outbursts of dwarf novae. The careful examination of quiescent disks of the same systems did not reveal any spiral structures in longer period DNe. Steeghs & Stehle (1999) argued that little evidence of spiral arms in the emission lines is expected in systems with low values of viscosity.

On the other hand, spiral arms related to 2:1 resonance can be found in systems with extremely low mass ratio $q < 0.1$ as originally was predicted by Lin & Papaloizou (1979). The bounce-back systems and related to them, WZ Sge stars, are examples of such objects. The long outburst recur-

rence time in WZ Sge systems is probably explained by a very low viscosity in their accretion disks, yet spiral arms can be observed permanently in quiescent bounce-back systems in which, on one side there is a massive WD, which gained mass during a long accretion history, and on another side there is a late-type brown dwarf, providing a mass ratio of ≤ 0.06 . Fig.4 (bottom, left) depicts a synthetic Doppler map constructed from a model accretion disk that is shown on the bottom right panel. The latter was calculated with the binary system parameters derived above by using smooth particle hydrodynamics according to Murray (1996); Kunze et al. (1997, and references therein). The artificial doppler map reproduces the observed map in a case when there is a brightness excess within spiral arms. Most of the disk particles are on periodic orbits, which are most favorable from the point-of-view of viscosity. However, the resonance dispatches some particles onto aperiodic orbits creating viscosity perturbations, which will create excess of heat. A slightly different interpretation of spiral arm brightness is offered by Ogilvie (2002). The mechanism is not very well established, but it is natural to assume that in these regions there will be excess emission.

5. Cyclic brightenings.

Figure 5 displays the light curve of SDSS 1238 obtained in 2007. In general, the object shows an identical behavior to previous years, as described by Zharikov et al. (2006). There are two distinct types of variability: a long-term variability (LTV), lasting more than 8h, and a short-term variability with a period corresponding to half the orbital period. Follow-up observations during 2008 and 2009 confirm a steady presence of both types of variability in the light curve (Fig.6). Continuous observations during about 15 hours obtained on 22/03/2007 (HJD 2454182.15-2544182.60, Fig.7) allowed us to observe two consecutive *brightenings* and, thus to determine their recurrence time directly (~ 9 h). Zharikov et al. (2006) demonstrated that *brightenings* occurred cyclically with periods in between 8 and 12 hours, however it was not possible to establish if the phenomenon was strictly periodic or not. Armed with more data, and the advantage of detecting consecutive events by employing multi-longitude observations, we performed a simple period search. The period analysis of all data obtained during 2007, based on a discrete Fourier transform method (Deeming 1975), results in a strong peak at a frequency $f_{\text{LTV}} = 2.59 \text{ day}^{-1}$ with FWHM of 0.1. This conforms with the period of $P_{\text{LTV}} = 9.28 \pm 0.36 \text{ h} \approx 7P_{\text{orb}}$ (Fig.8). However, the data folded with this period looks messy because, apparently, some re-brightenings happen with a different cycle period. It shows that the large uncertainty in the period value is not just a result of a scarce amount of data, or its uneven distribution, but that the *brightenings* are not strictly periodic in long timescales. The peak $2 \times f_{\text{orb}} = 35.76 \text{ day}^{-1}$, corresponding to the half of the orbital period, $P_{\text{orb}}/2 = 40.3 \text{ min}$, is also present in the power spectrum. There are some additional peaks which are one-day aliases or a combination of high harmonics of f_{LTV} with $2 \times f_{\text{orb}}$. We have repeated the same analysis for the data obtained only within HJD 2454177.1-2544185.6, when we observed the object with small observational gaps. The result of the analysis of periodicity for this selection is presented in Fig.9. The strongest peak in the power spectrum appears at a frequency corresponding to $P_{\text{LTV}}^* = 9.34(26) \text{ h}$. The light curve folded with this period is coherent during the considered time

(Fig.9), i.e macro-profile of the *brightenings* (the rise, the peak, the declining slope and minimum duration) repeats itself with high accuracy and, if not for the high-frequency modulation also present in the light curve, the folded curves would concur. Combining the entire available data obtained during the 2004 — 2009 observational runs does not permit a determination of a single period with which the entire data set can be folded. Clearly, the LTV modulation is not strictly periodic, but probably maintains coherence in a time scale of several weeks and certainly has a cyclic nature.

The long-term variability (*the brightenings*) presents a fast rise in the object brightness of up to 0.4-0.6 mag, lasting about half the orbital period (~ 0.7 h) with the brightness falling back to the quiescence level during the next 4.4-4.6 h (Fig. 7). After that, the object remains in quiescence during about another 4 hours. The brightness increases at a rate of ~ 0.75 mag/h, and the falling rate is about ~ 0.10 mag/h. Sometimes, the rise in the brightness happens more slowly and lasts until almost one full orbital period (Fig.5 nights: 156, 179).

A short-term variability is clearly present during *the brightenings*. The amplitude of the short-term variability depends strongly on the phase of *brightenings*. The amplitude is larger then the total brightness increases and falls, sometimes practically disappearing, between the *brightenings* (Figs. 5, 6, 7). Curiously, when the LTV is coherent, the signal at double orbital frequency decreases and a beat frequency between the LTV and $2 \times f_{\text{orb}}$ becomes dominant in the range of frequencies around 36 cycles/day. Removing LTV has little effect, because this does affect the frequency modulation but not the amplitude modulation. The strong relation between LTV cycle coherence and the strength of $2 \times f_{\text{orb}}$ modulation attests that these two phenomena are physically linked in more than a simple amplitude correlation. We suspect that the *brightenings* and formation of spiral arms in the disk are the result of the same process, but its cyclic nature remains unclear.

6. Discussion and conclusions

In recent years, a number of objects were discovered, mostly thanks to the Sloan Digital Sky Survey, which can be characterized as WZ Sge type CVs in quiescence, judging by their $\sim 80 - 85$ min periods, spectral appearance and lack of SU UMa style outburst activity. Currently, there are about 20 objects with similar characteristics which were selected from the SDSS lists. Three such objects are GW Lib, V455 And and SDSS0804, which underwent a typical WZ Sge type super-outburst in 2006-2007, confirming the correct assessment of their nature from their behavior in quiescence. But unlike classical WZ Sge stars, some of them differ by the presence of permanent double-humps per orbital period in the light curve. The significance of the double-humped light curve lies in the assumption that it is produced by the spiral structure in the accretion disk. The spiral arms in accretion disks have been detected before by means of Doppler tomography in long period systems only during DN outburst. We are not aware of any reports of double-humped light curves during these detections. Double-humped light curves have previously came to attention, as they were detected during super-outbursts of WZ Sge. It was soon suggested that they are result

of 2:1 resonance (Osaki & Meyer 2002; Patterson et al. 2002), as one of the possibilities. Also spirals arms are formed in the accretion disk of the WZ Sge undergoing super-outburst (Steehls 2004), because, according to our hypothesis WZ Sge accretion disk reaches the resonance radius only during super-outburst. Nevertheless, the spiral structure has been observed persistently along with the double-humped light curve in two similar short-period systems, SDSS 0804 and SDSS 1238 in quiescence. We assume that the spiral structure formed in low viscosity, quiescent disks is a result of distortion of the disk by the 2:1 resonance. The 2:1 resonance may happen only in the accretion disk of a system with extreme mass ratio of $q \leq 0.1$. Such mass ratio is achieved only in systems known as bounce-backed or, in other words, systems which have reached a minimum period of ≈ 80 min and have turned to slightly longer periods according to Paczynski (1981). It is expected that bounce-back systems are numerous (Kolb & Baraffe 1999), but until recently very few candidates have been found. The SDSS helped to uncover a large number of new CVs, with new interesting features (Gänsicke et al. 2009). Among them, there is a number of short period systems, some of which turned out to belong to the long-sought bounce-back systems (Littlefair et al. 2008; Mennickent & Diaz 2002).

We have unveiled a brown dwarf secondary in SDSS 1238, probably as late as L4, thus providing strong evidence that this object is a real bounce-back system. We also estimated parameters of the WD. The best fit to the SED converges if the primary is a massive $M_{WD} \approx 1.0 M_{\odot}$ white dwarf with a $T_{WD} = 12\,000$ K temperature. Both numbers seem plausible since the system is very old and the WD is expected to be relatively massive and cool. These findings provide further support to our claim that by simply observing a permanent double humped light curves one can identify an evolved, bounce-back systems instead of using other complicated methods.

It is important to note that SDSS 1238 has another peculiarity, which Zharikov et al. (2006) termed as *brightenings*. There was only one other system known to exhibit *brightenings*, namely SDSS 0804, but since it underwent a super-outburst in 2006, its photometric behavior has drastically changed. The *brightenings* shortly detected by Szkody et al. (2006) in SDSS 0804 before the super-outburst have been replaced by: a) *the mini-outburst* activity with permanent presence of the double-humped light curve of constant amplitude (Zharikov et al. 2008) and by: b) a 12.6 min period, probably corresponding to pulsation activity of the WD (Pavlenko et al. 2007). Therefore, at present, SDSS 1238 is the only object known to show *brightenings*. It greatly complicates the study of this phenomenon. Based on new multi-longitude continuous monitoring, we demonstrated here that the *brightenings* are of cyclic nature with a recurrence time of ≈ 9 hours and they are probably coherent over several cycles. There seem to be strong correlation between *brightenings* cycles and the amplitude of double-hump periodic variability. This is believed to be the result of spiral arms in the accretion disk of bounce-back systems with an extreme mass ratio, in which accretion disk extends beyond a 2:1 resonance radius. The tomogram of a simulated accretion disk in the regime of resonance, closely resembles the observed one and supports this hypothesis. The formation of a spiral structure in the disk can be accounted by the appearance of double humps in the light curve, but it can not be the reason of increased brightness of the disk. The disk brightness

directly depends on the mass transfer rate and its change should probably reflect change in mass transfer. No readily explanation is available as to why that rate can be variable and cyclical, but possible speculations include counteraction: a) to the heating of the secondary by *brightenings*, or b) to tidal interaction between the secondary with the resonance attaining accretion disk.

This work was supported in part by DGAPA/PAPIIT projects IN109209 and IN102607.

REFERENCES

- Aviles, A., Zharikov, S., Tovmassian, G., et al., 2010, in preparation.
- Baba, H., et al. 2002, PASJ, 54, L7
- Close L.M., et al., 2003, ApJ, 587, 407
- Deeming, T. J. 1975, Ap&SS, 36, 137
- Gänsicke, B. T., et al. 2009, MNRAS, 397, 2170
- Heemskerk, M. H. M. 1994, A&A, 288, 807
- Howell, S. B., Adamson, A., & Steeghs, D. 2003, A&A, 399, 219
- Knigge, C. 2006, MNRAS, 373, 484
- Kolb, U., & Baraffe, I. 1999, MNRAS, 309, 1034
- Kunze, S., Speith, R., & Riffert, H. 1997, MNRAS, 289, 889
- Kunze, S., & Speith, R. 2005, The Astrophysics of Cataclysmic Variables and Related Objects , 330, 389
- Kurucz, R. 1993, ATLAS9 Stellar Atmosphere Programs and 2 km/s grid. Kurucz CD-ROM No. 13. Cambridge, Mass.: Smithsonian Astrophysical Observatory, 1993., 13
- Lin, D. N. C., & Papaloizou, J. 1979, MNRAS, 186, 799
- Littlefair, S. P., Dhillon, V. S., Marsh, T. R., Gänsicke, B. T., Southworth, J., Baraffe, I., Watson, C. A., & Copperwheat, C. 2008, MNRAS, 388, 1582
- Lynden-Bell, D. 1969, Nature, 223, 690
- Matsuda, T., Sekino, N., Shima, E., Sawada, K., & Spruit, H. 1990, A&A, 235, 211
- Martini, P., Persson, S. E., Murphy, D. C., Birk, C., Shectman, S. A., Gunnels, S. M., & Koch, E. 2004, Proc. SPIE, 5492, 1653

- Marsh, T.R., Horne, K. 1988, MNRAS, 235, 269
- McLean, I. S., McGovern, M. R., Burgasser, A. J., Kirkpatrick, J. D., Prato, L., & Kim, S. S. 2003, ApJ, 596, 561
- McLean, I. S., Prato, L., McGovern, M. R., Burgasser, A. J., Kirkpatrick, J. D., Rice, E. L., & Kim, S. S. 2007, ApJ, 658, 1217
- Mennickent, R. E., & Diaz, M. P. 2002, MNRAS, 336, 767
- Murray, J. R. 1996, MNRAS, 279, 402
- Nauenberg, M. 1972, ApJ, 175, 417
- Osaki, Y., & Meyer, F. 2002, A&A, 383, 574
- Ogilvie, G. I. 2002, MNRAS, 330, 937
- Paczynski, B. 1981, Acta Astronomica, 31, 1
- Patterson, J., et al. 2002, PASP, 114, 721
- Patterson, J., et al. 2002, PASP, 114, 1364
- Pavlenko, E., et al. 2007, 15th European Workshop on White Dwarfs, 372, 511
- Persson, S. E., Murphy, D. C., Krzeminski, W., Roth, M., & Rieke, M. J. 1998, AJ, 116, 2475
- Piskunov, N. E. 1992, Stellar Magnetism, 92
- Sawada, K., Matsuda, T., & Hachisu, I. 1986a, MNRAS, 221, 679
- Sawada, K., Matsuda, T., & Hachisu, I. 1986b, MNRAS, 219, 75
- Steehls, D., & Stehle, R. 1999, MNRAS, 307, 99
- Steehls, D. 2001, Astrotomography, Indirect Imaging Methods in Observational Astronomy, 573, 45
- Steehls, D. 2004, Revista Mexicana de Astronomia y Astrofisica Conference Series, 20, 178
- Stehle, R. 1999, MNRAS, 304, 687
- Szkody, P., et al. 2003, AJ, 126, 1499
- Szkody, P., et al. 2006, AJ, 131, 973
- Tinney, C.G., Burgasser, A. J., Kirkpatrick, J. D. 2003, AJ, 126, 975
- Truss, M. R. 2007, MNRAS, 376, 89

- Southworth, J., Gänsicke, B. T., Marsh, T. R., de Martino, D., Hakala, P., Littlefair, S., Rodríguez-Gil, P., & Szkody, P. 2006, *MNRAS*, 373, 687
- Warner, B. 1995, *Cambridge Astrophysics Series*, 28
- Zharikov, S. V., Tovmassian, G. H., Napiwotzki, R., Michel, R., & Neustroev, V. 2006, *A&A*, 449, 645
- Zharikov, S. V., et al. 2008, *A&A*, 486, 505

Table 1: Log of time-resolved observations of SDSS J123813.73-033933.0 in V band

Date	HJD Start+ 2454000	Telescope	Exp.Time Num. of Integrations	Duration
Photometry				
25 Feb. 2007	156.832	1.5m/SPM/México	120s×160	5.3h
26 Feb. 2007	157.845	1.5m/SPM/México	120s×144	4.8h
15 Mar. 2007	174.756	1.5m/SPM/México	220s×95	5.8h
18 Mar. 2007	177.767	1.5m/SPM/México	170s×91	4.3h
19 Mar. 2007	178.716	1.5m/SPM/México	240s×108	7.2h
20 Mar. 2007	179.414	2m/Terksol/Russia	120s×118	3.9h
20 Mar. 2007	179.746	1.5m/SPM/México	160s×77	3.4h
20 Mar. 2007	180.290	2m/Terksol/Russia	120s×152	5.1h
21 Mar. 2007	181.169	2m/IAO/India	120s×135	7.5h
21 Mar. 2007	181.286	2m/Terksol/Russia	120s×210	7h
22 Mar. 2007	182.164	2m/IAO/India	120s×198	6.9h
22 Mar. 2007	182.302	2m/Terksol/Russia	120s×195	6.5h
22 Mar. 2007	182.435	0.8m/IAC80/Spain	270s×98	7.4h
25 Mar. 2007	185.032	2.1m/BOAO/Korea	135s×107	4.0h
25 Apr. 2007	216.696	0.8m/IAC80/Spain	200s×101	5.6h
27 Apr. 2007	218.648	0.8m/IAC80/Spain	200s×116	6.4h
09 Mar. 2008	535.904	1.5m/SPM/México	60s×150	2.5h
10 Mar. 2008	536.882	1.5m/SPM/México	60s×200	3.3h
11 Mar. 2008	537.889	1.5m/SPM/México	60s×170	2.8h
27 Feb. 2009	890.826	1.5m/SPM/México	60s×184	3.1h
28 Feb. 2009	891.814	1.5m/SPM/México	60s×227	3.8h
01 Mar. 2009	892.851	1.5m/SPM/México	60s×218	3.6h

Table 2: Log of time-resolved spectroscopic observations of SDSS J123813.73-033933.0

Date	HJD Start+ 2454000	Telescope	Exp.Time	Duration Num. of Integrations
Spectroscopy				
24 Jan. 2009	855.99	2.1m/SPM/México	486s×7	0.52h
25 Jan. 2009	856.96	2.1m/SPM/México	486s×17	2.43h
26 Jan. 2009	857.90	2.1m/SPM/México	486s×20	2.69h
27 Jan. 2009	856.96	2.1m/SPM/México	486s×10	1.2h

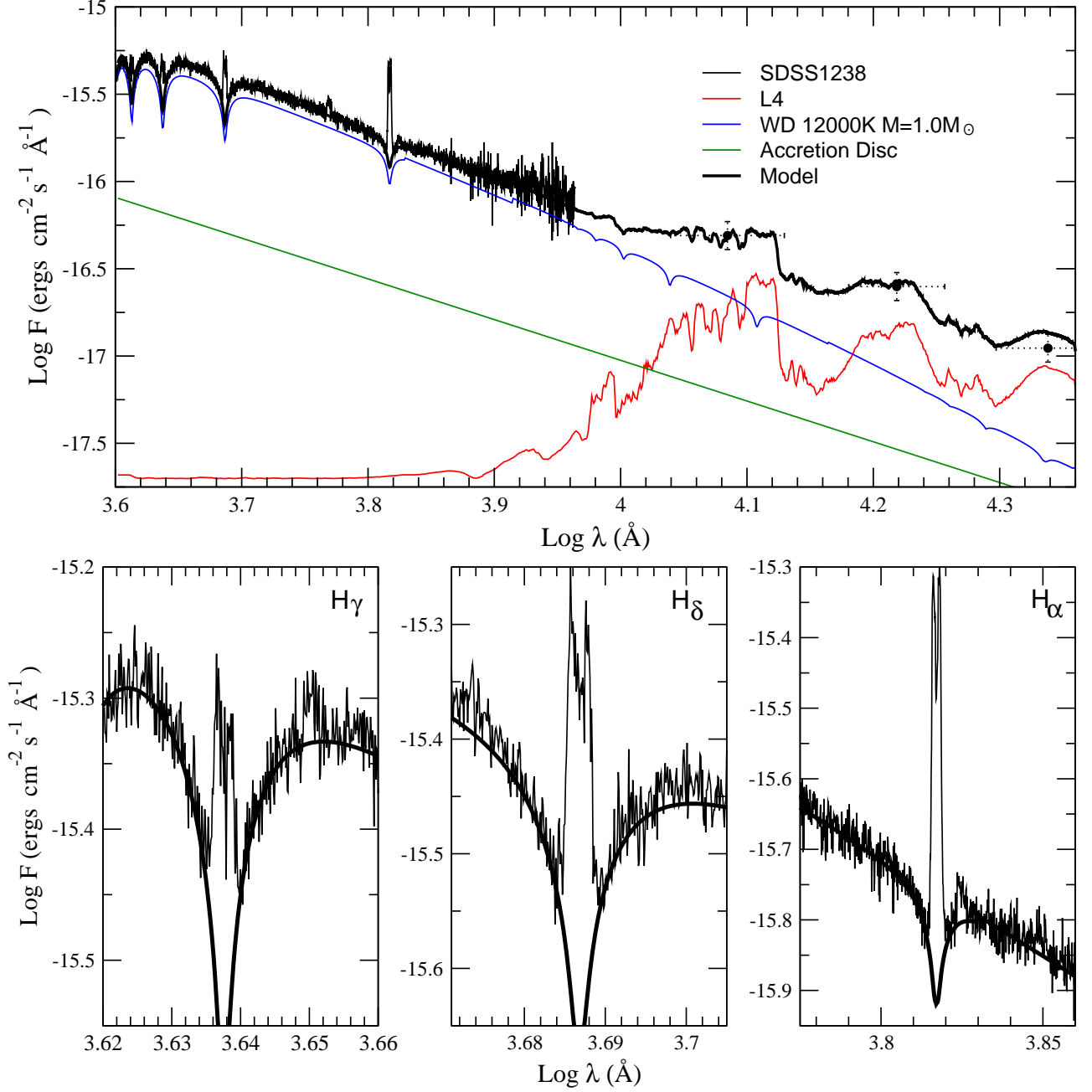


Fig. 1.— The spectral energy distribution of SDSS 1238 and the result of the model fit (top). Spectrum fragments around H_{γ} , H_{δ} and H_{α} lines are shown in bottom panels.

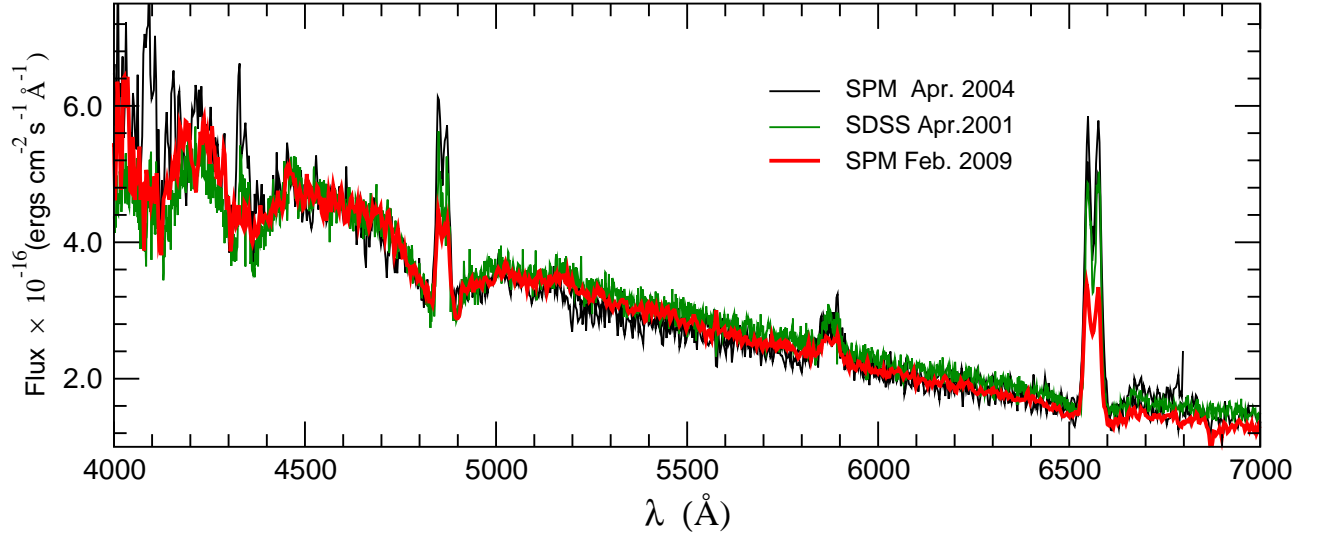


Fig. 2.— The low-resolution time-average spectra of SDSS1238 obtained in different epochs.

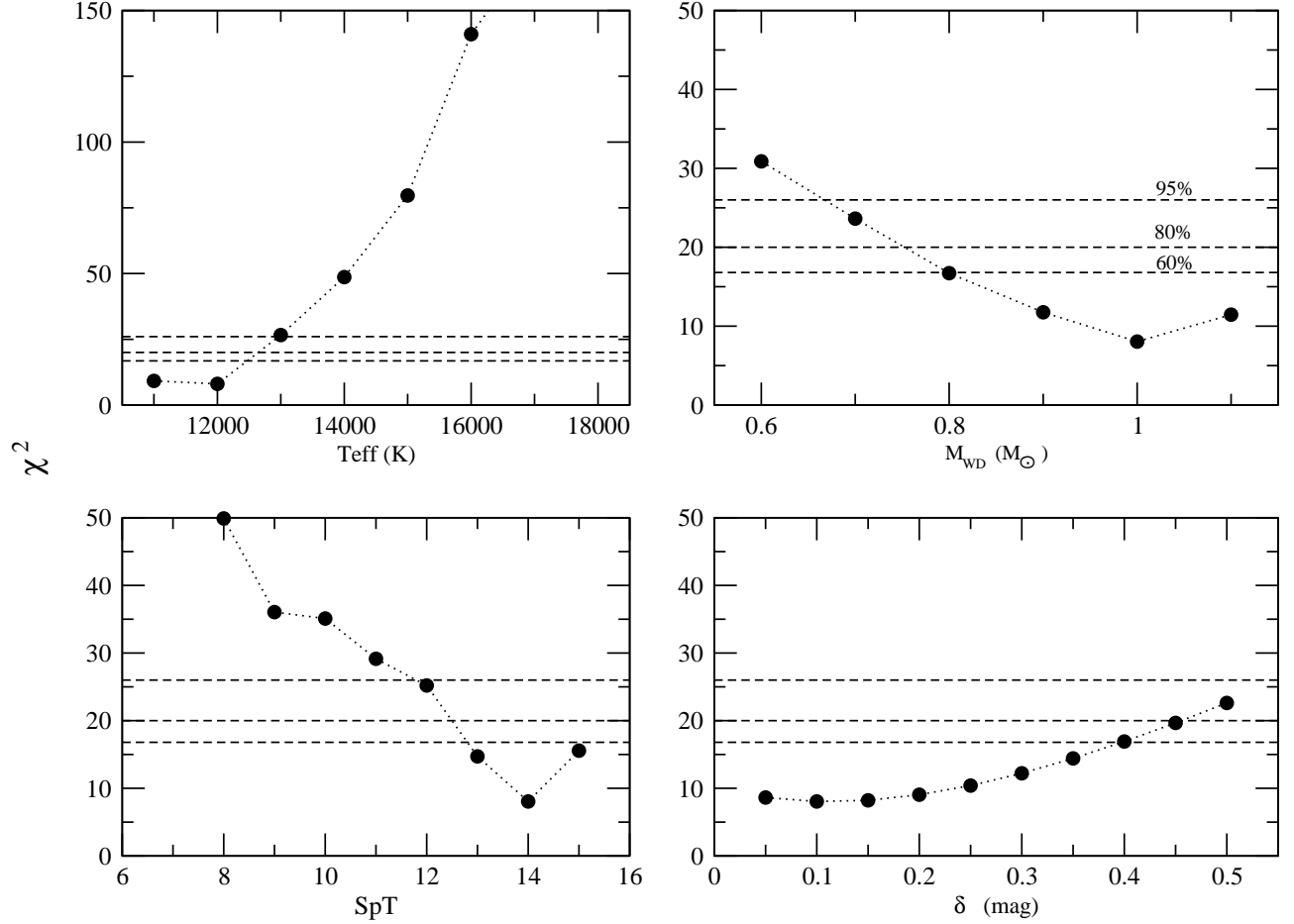


Fig. 3.— χ^2 vs parameters of the fit, where T_{eff} is an effective temperature of the primary WD, M_{WD} is a mass of the WD, SpT is a spectral type of the secondary (from M6V/SpT=6 to L6/SpT=16) and δ is a ratio between accretion disk and WD contribution in the continuum flux of the SDSS1238 in the V band. The formal confidence levels by the fit are presented by dashed lines. The numbers at the dashed lines are a probability to reject a model with χ^2 above corresponding line.

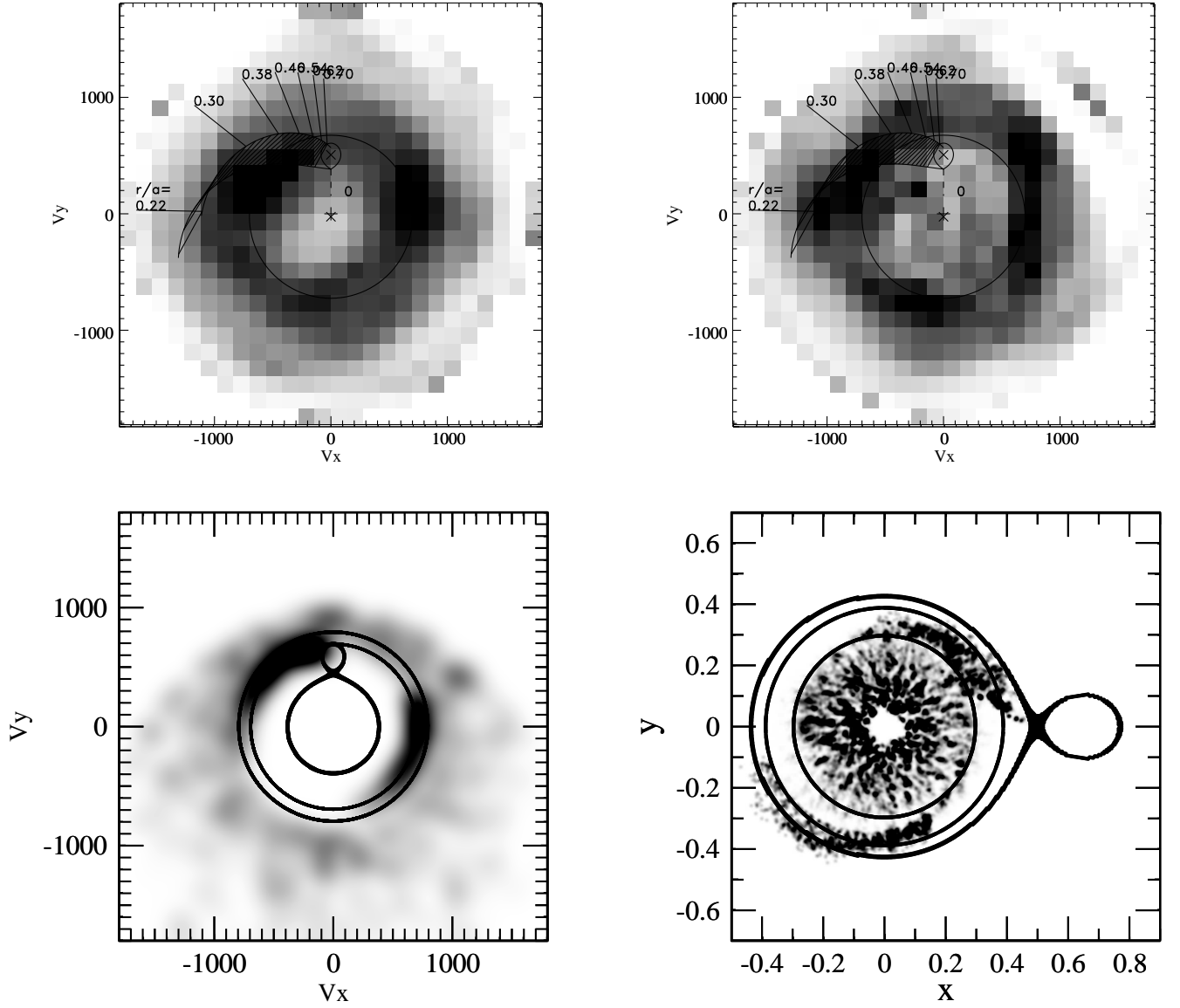


Fig. 4.— top) H_α Doppler maps constructed on all data obtained in the 2004 (left) and 2009 (right) yy. The circle show the velocity at 2:1 resonance radius. bottom) The synthetic Doppler map (left) obtained from a model accretion disk (right) for the system with $M_{WD} = 1.0M_\odot$ and $q = 0.05$. The circles correspond to 2:1 and 3:1 resonance radiuses.

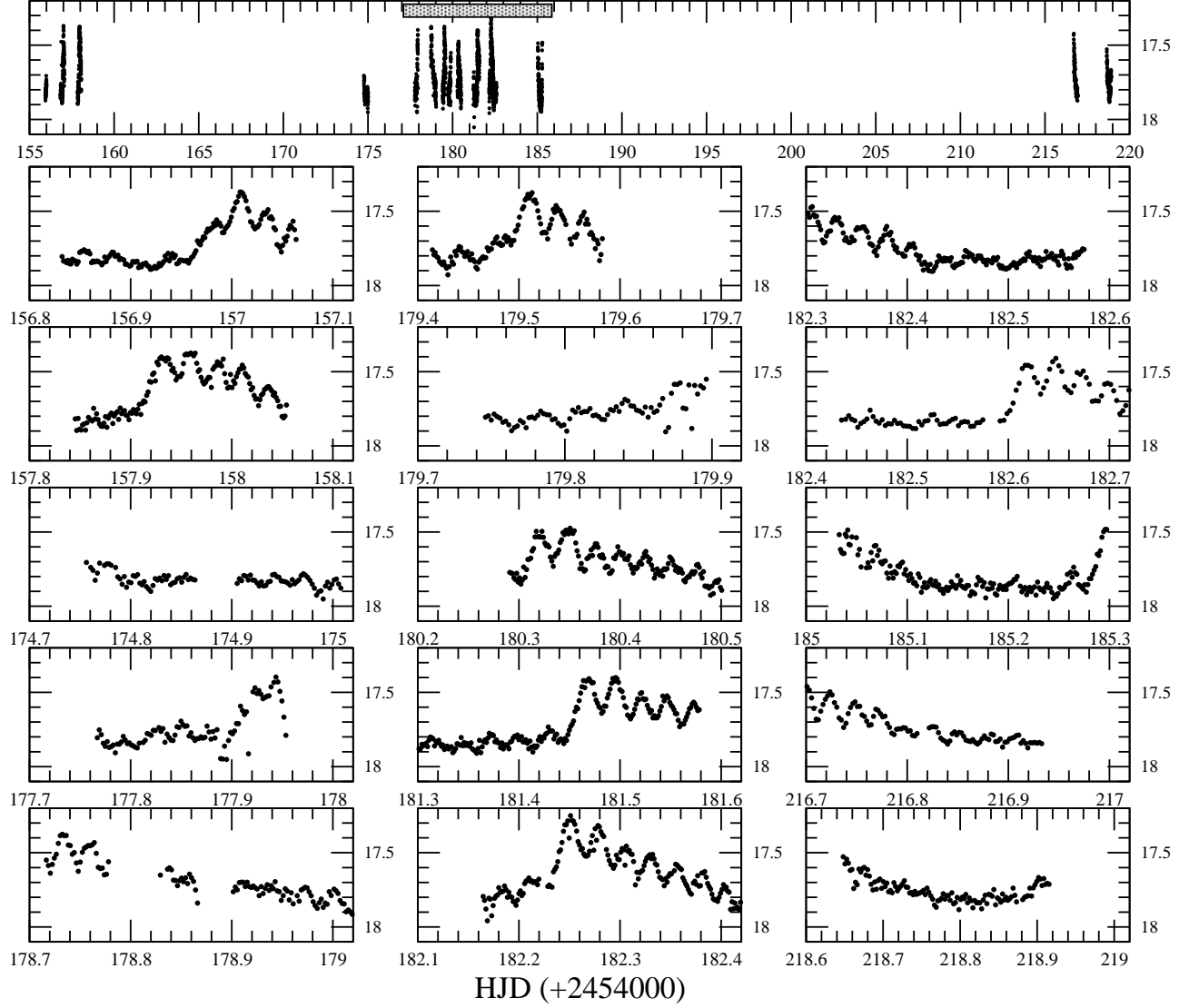


Fig. 5.— The light curve of SDSS 1238 in V band obtained in the 2007 year. Each night is presented in a separate panel.

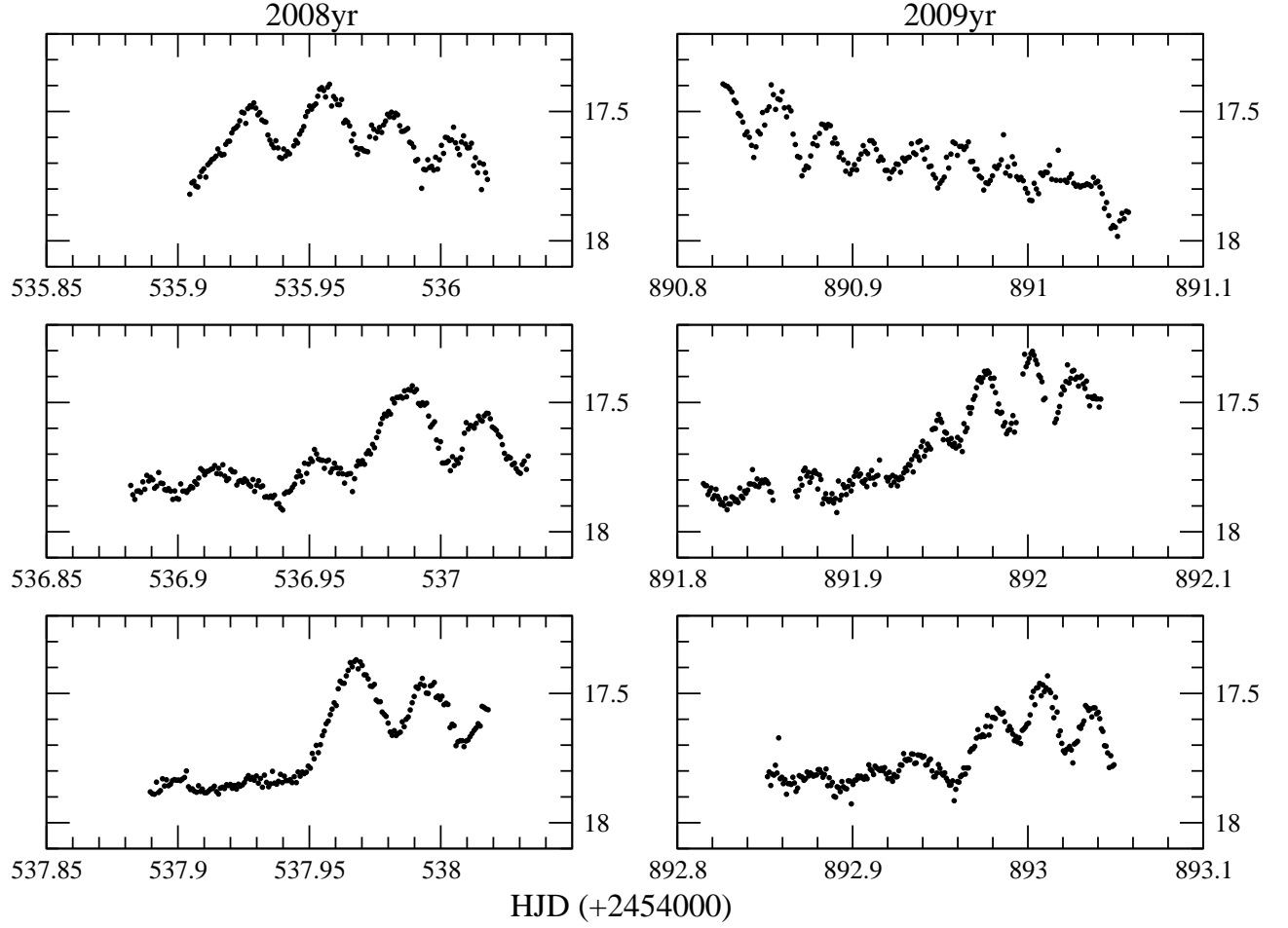


Fig. 6.— The light curve of SDSS 1238 in V band obtained in 2008 and 2009 yy. Each night is presented in a separate panel.

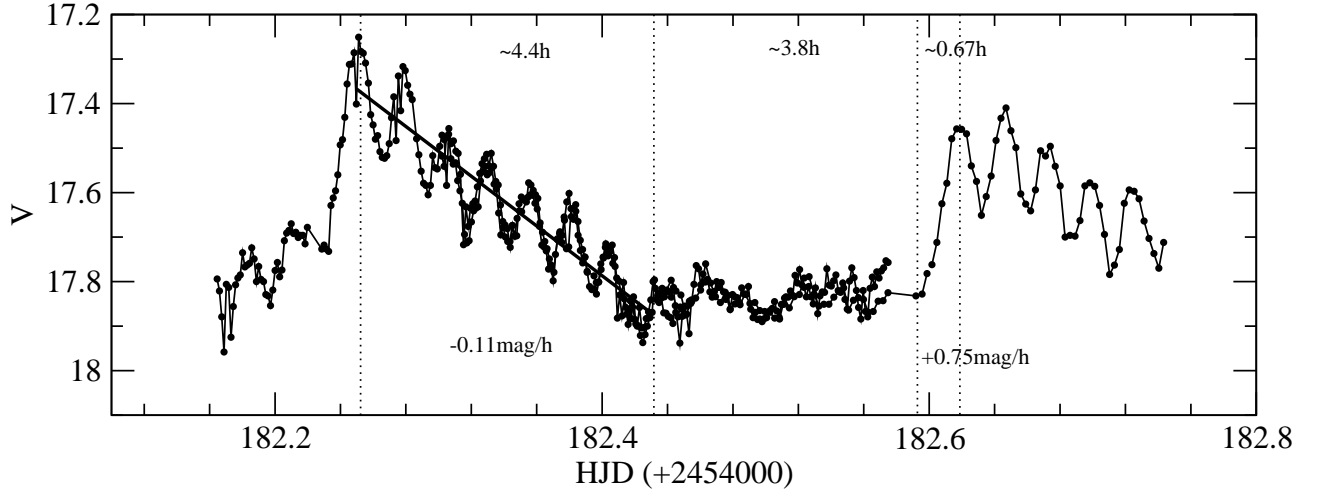


Fig. 7.— The light curve of SDSS 1238 in V band obtained during about 15 hours continuous observations in HJD 2454182. Vertical dashed lines select different phases of the long-term variability (LTV). The numbers in the top of the figure are approximately durations for each marked phase of LTV and the numbers in the bottom are corresponding rates of the magnitude change during fading and increasing of the object brightness.

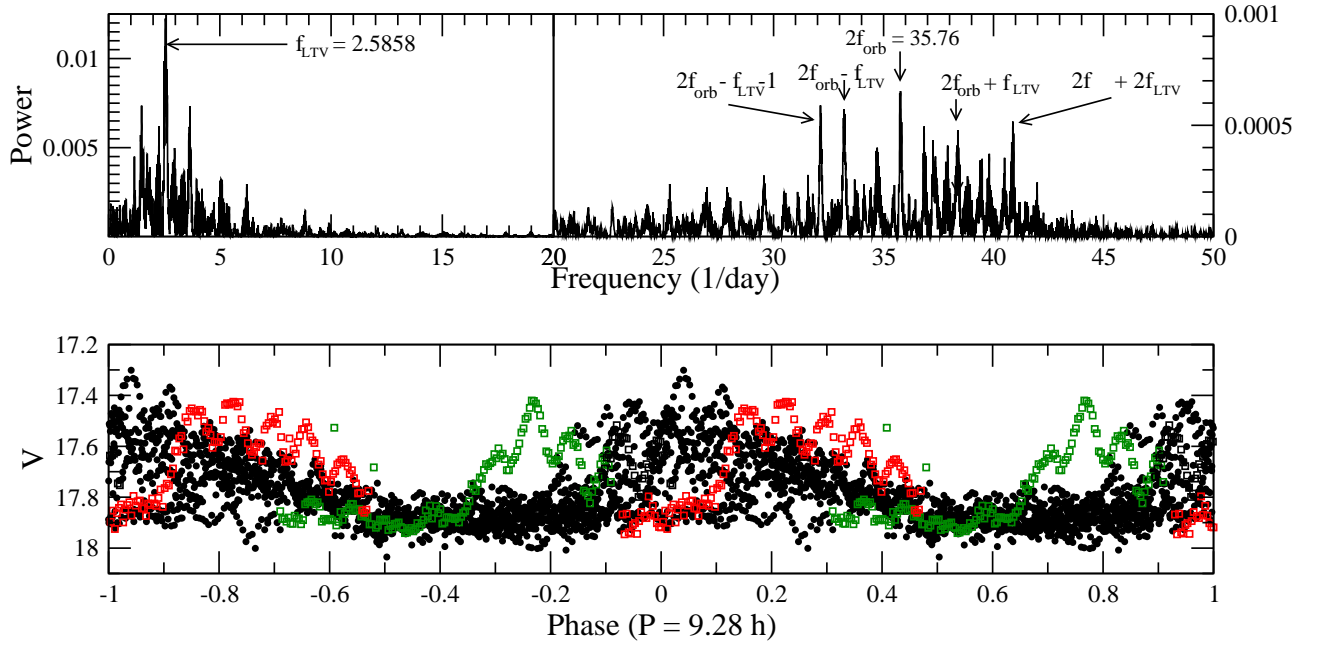


Fig. 8.— top) The power spectrum of the all photometric data presented in the top panel of Fig.6. bottom) The light curve comprised of the all data folded on $P = 9.28$ h. The open color points show *brightenings* with maximal displacement in the light curve folded on $P = 9.28$ h.

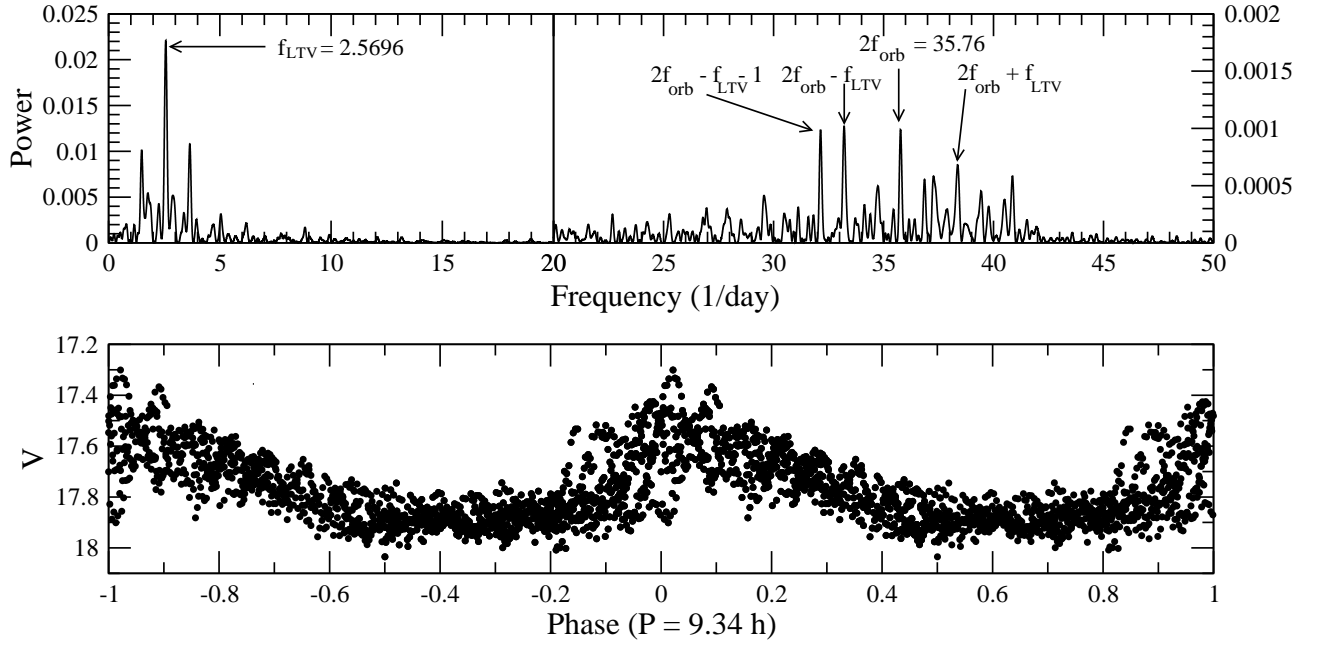


Fig. 9.— top) The power spectrum of the data obtained in the period of HJD 2454177.1-2454185.6 (see Fig.6). bottom) The light curve comprised of the selected data from the period of HJD 2454177.1-2454185.6 folded on $P = 9.34\text{h}$ period.